Heliyon 10 (2024) e25348

Contents lists available at ScienceDirect

Heliyon

journal homepage: www.cell.com/heliyon

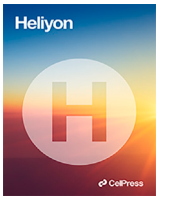

Research article

Mathematical model for the plastic flow and ductile fracture of polycrystalline solids

Miguel Lagos [a,*], César Retamal [a], Rodrigo Valle [a], Rodrigo Paredes [b]

[a] Facultad de Ingeniería, Universidad de Talca, Campus Los Niches, Curicó, Chile
[b] Facultad de Ingeniería, Universidad Finis Terrae, Av. Pedro de Valdivia 1509, Providencia, Santiago, Chile

ARTICLE INFO

Keywords:
Grain boundary sliding
Polycrystal plasticity modelling
Plastic flow properties
Residual stress
Ductile fracture
Strain to failure

ABSTRACT

It is mathematically shown that ductile fracture after finite plastic strain is a necessary consequence of the polycrystalline nature of the materials. A closed–form equation for the plastic strain to fracture of a fine–grained polycrystal with no voids is derived. The mathematical model for the plastic deformation is grounded on the physical hypothesis that adjacent grains slide with a relative velocity proportional to the local shear stress resolved in the plane of the shared grain boundary, when exceeds a finite threshold. Hence plastic flow is governed predominantly by the in–plane shear forces making grain boundaries to slide, and the induced local forces responsible for the continuous grain reshaping are much weaker. The process is shown to produce a monotonic hydrostatic pressure variation with strain that precludes a stationary flow. The hydrostatic pressure dependence on strain has two solutions. One of them leads to superplasticity, the other one is shown to diverge logarithmically at a finite fracture strain and then represents ductile behaviour. Emphasis is done in the mathematical aspects of the deformation of the polycrystal up to the initiation of fracture. Although theoretical predictions agree well with mechanical tests of commercial alloys, technical issues like the effects of the presence and evolution of porosity and other imperfections, or how fracture evolves after initiation are left for a more specific communication.

1. Introduction

Resorting to a very general model for the structure of the solid, we demonstrate in what follows that fine grained polycrystalline materials, with no voids or cracks, are not able of steady plastic flow, no matter the strength of the forces involved, and should finally collapse. Continued plastic deformation inevitably makes crystalline solids to undergo either brittle, ductile or superplastic fracture. In particular, the ductile flow mode is characterized by fracture occurring when the plastic strain reaches a precisely defined finite value. The model may be perceived as fairly idealized because does not consider the presence, formation and evolution of voids, but shows that these defects are not necessarily involved in the initiation of ductile fracture. It is shown that fracture is a necessary step of the plastic deformation of a polycrystalline solid, even of a perfect one.

The ideas presented below confront the custom approaches to fracture. To date, the nucleation, growth and coalescence of internal voids and cracks have been taken as the dominant fracture mechanism of ductile solids subjected to strong enough stress fields. However, although void rapid evolution and fracture development show strong correlation, the causal aspect is not obvious.

* Corresponding author.
E-mail addresses: mlagos@utalca.cl (M. Lagos), ceretamal@utalca.cl (C. Retamal), r.vallefuentes@gmail.com (R. Valle), raparede@dcc.uchile.cl (R. Paredes).

https://doi.org/10.1016/j.heliyon.2024.e25348
Received 10 July 2023; Received in revised form 11 January 2024; Accepted 25 January 2024

Available online 30 January 2024

Whatever be the ultimate cause of ductile fracture, it may be expected to proceed by successive local collapses involving different small portions of the material which sequentially reach the fracture conditions at different places inside the material. In this picture the ultimate causes of fracture are prior to the accelerated development of voids and cracks, since these should be identified with the early local fractures mentioned before. Naturally, pre–existent defects may precipitate early fracture. As noted long ago by Orowan [1], fracture is not a single physical phenomenon, there are several essentially different processes that may lead to the disintegration of a body by the action of mechanical forces. The present point is why polycrystalline solids do not steadily flow under strong enough forces and break after a quite small plastic deformation. Of less importance is here what of the specific microscopic local rupture processes has the dominant role in a specific situation, or whether they work together or in a sequence during the fracture.

It will be demonstrated of key importance the observation that the faceted nature of the crystalline grains constituting the polycrystal has a determinant effect in the plastic flow, no matter how small the grains may be. At a scale much larger than the grain size, polycrystalline matter lacks symmetry constrictions and periodicity, and displays same average packing and properties in all directions, and over its whole extension. Despite this, assimilating an even very fine grained polycrystal to an homogeneous and isotropic continuum may lead to gross errors, no matter the scale, when dealing with it as a dynamical medium. It has been shown in a previous paper [2,3], and will be reviewed here, that the faceted nature of the structural constituents of a polycrystal determines that the force fields governing their plastic flow yield $\nabla \cdot \vec{v} \neq 0$, where $\vec{v}$ is the velocity field of the material continuum. This means that flow makes the specific volume to vary, and hence the consequent rapid build up of the hydrostatic pressure. Grain elasticity in polycrystalline solids allows for some density variation, and hence the medium can flow up to some extent, yielding ductile behaviour. However, the consequent pressure build up influences strongly the ongoing deformation, which cannot be steady, and finally produces fracture. The theory predicts two possible regimes of deformation, one of them can be identified with superplasticity and the other one with normal ductile deformation because exhibits a well defined fracture strain at which the hydrostatic pressure has a logarithmic divergence.

Although the point is reviewed in precise terms later on, the dynamical effect of the faceted nature of the constituents of the flowing medium deserves to advance a physical explanation. The sliding of two contiguous grains is necessarily driven by the shear force field resolved in the plane of the grain surface shared by the two grains. However, if the normal to the common surface of the grains gets close enough to a principal direction of the stress tensor, then the resolved shear stress becomes smaller than the threshold stress τ_c for grain sliding, regardless the strength of the applied forces. Hence grains whose boundaries have normals in solid angles around the principal directions are impeded to slide (see Fig. 3a of Ref. [4]). This introduces a non–analytic anisotropy in the motion of the grains which is shown to be inconsistent with the equation of local conservation of mass density $\nabla \cdot \vec{v} = 0$ [2,4,5,3].

1.1. Fracture evolution

Although the subject here is fracture initiation, subsequent evolution occupies considerable space in the literature and deserves some words. Tensile tests combining in situ X–ray microtomography with scanning electron microscopy (SEM) dramatically show the rapid increase of void number and size when fracture comes to the fore. [6–10]. However, as explained before, according to the ideas put forward here this phenomenon concerns more to **how** fracture evolves than **why** it takes place. Anyway the apparent importance of the problem in technical grounds has motivated a great deal of effort. The pioneer work of Griffith [11] on the tensile strength of glass, who postulated the presence of small pre–existent cracks that concentrate stresses when the material is loaded, and Irwin [12] and Orowan [1], who extended the idea to ductile solids, has initiated a rather fundamental investigation line devoted to study the breaking of solid materials from the atomic point of view. Brittle behaviour is ascribed to the ability of the stressed crack tips to propagate conserving their atomically sharp edges, while in ductile solids the tip of the crack blunts, broadens and flows, demanding increasing effort to make it progress. References [13], [14] and [15] show the general spirit of this research line and the work [16] gives a rather complete review.

A more phenomenologycal approach, more connected with the technical aspects of plastic yield is the one introduced by Gurson [17] and subsequently modified by other authors [18–20], which derive an analytical expression for the yield function in terms of the void concentration. Spherical and cylindrical voids are assumed in a continuous plastic matrix obeying the von Mises yield criterion and Lévy–Mises flow equations [21]. Emphasis is not in fracture, but in plastic yield. Other models [22–26] develop yield criteria and flow rules for the evolution under stress of porous ductile materials, showing the role of void nucleation, growth and coalescence in plastic yield.

The main ductile fracture criteria are discussed by Li et al. [27], which study their reliability by comparing predictions with the mechanical test of an aluminium alloy in a variety of conditions. In a recent paper Noell et al. [28] dissent of the widely accepted ideas and assert that fracture is not controlled by just void nucleation, growth and coalescence. Rather, the rupture process may be due to as many as seven different mechanisms, which are not necessarily independent or exclusive, and can work in sequence. Examples are intervoid necking, the nucleation of voids in a shear band, and void sheeting. However, most models link fracture with void nucleation and evolution. The Rosselier model describes the damage due to the plastic growth of cavities in metals. Cracking and ductile rupture is modelized by elastoplastic or viscoplastic processes with isotropic work hardening [29–32].

We do not extend the theoretical approach presented here to incorporate porosity because we wish to stress that ductile fracture of fine grained quality materials is caused by their polyhedral nature. The development of voids pertains to the fracture process rather than to its cause. The work of Khan, Yu and Liu [33–35] has a particular connection with the results presented here because these authors provide empirical evidence of the importance of the hydrostatic pressure in the fracture process. On the basis of the experimental data on titanium and aluminium alloys, taken with controlled negative and positive superimposed hydrostatic

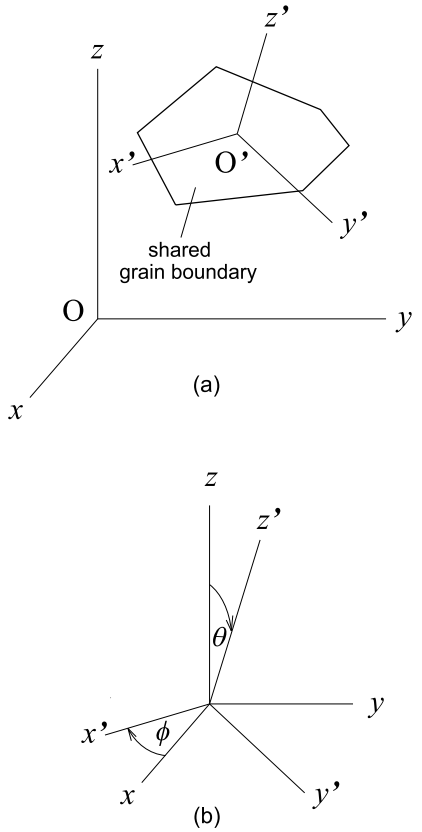

Fig. 1. (a) Schematic view of the grain boundary shared by two adjacent grains, showing the local frame of reference $(x'y'z')$ having the $x'y'$ plane in the grain boundary plane, and the main frame of reference (xyz) with the axes along the principal directions of the stress tensor. (b) The principal and local frames of reference, showing the Euler angles θ and ϕ.

pressures, they establish a phenomenological fracture criterion using the magnitude of stress vector and the first invariant of stress tensor. The capital role played by the first invariant, the hydrostatic pressure, in our scheme has been commented before.

2. The model and force law

The model for the plastic flow of a polycrystalline solid already has been extensively studied in the context of superplasticity [2], but is expected to hold equally well for normal ductile solids [3]. The two flow regimes, superplastic and plastic, correspond to two different solutions derived from the same theoretical framework. A brief review of the physical basis of the model and the resulting general theoretical scheme is given next to make clear the conditions for the occurrence of either superplastic or normal ductile behaviour.

The plastic deformation of a fine grained polycrystalline solid is modelled as a flowing continuum of random irregular polyhedra of different shapes and sizes, representing grains, which share faces. The model is essentially the same as the one introduced in Ref. [2] and refined in [4]. Grains can move over long paths by sliding along the shared surfaces, or grain boundaries, accommodating effortlessly their shapes to preserve matter continuity. Certainly, grain shape accommodation demands some effort, but it is assumed much smaller than the one required for grain sliding. In other words, the shear stress involved in the relative sliding of two grains is greater than the critical resolved shear stress (CRSS) demanded by slip deformation of the crystallites.

The macroscopic laws connecting the evolution in time of the strain tensor ε_{ij} with the stress tensor σ_{ij}, $i,j = x,y,z$, induced by the externally applied forces, are determined by the forces exerted between the many pairs of adjacent grains and their relative motions. Hence the dynamical analysis has to go first to the scale of grains. In this spirit we define a local frame of reference $(x'y'z')$ with the $x'y'$ plane coincident with the boundary between two adjacent grains, as is represented in Fig. 1. The total shear stress in the boundary plane shared by the two adjacent grains then reads

$$\tau_{z'} = (\sigma^2_{x'z'} + \sigma^2_{y'z'})^{1/2},$$

where $\sigma_{i'j'}$, $i',j' = x',y',z'$, stands for the components of the stress tensor in this local coordinate system. There is strong evidence that the sliding relative speed $|\Delta\vec{v}|$ of two adjacent grains obeys a linear law of the general form $|\Delta\vec{v}| = Q(\tau_{z'} - \tau_c)$ for $\tau_{z'} > \tau_c$ in plastic deformation [2,3,36–38], and vanishes when the critical shear stress τ_c is not reached. Here Q is a proportionality coefficient. Fig. 2 expresses this in a graphical way.

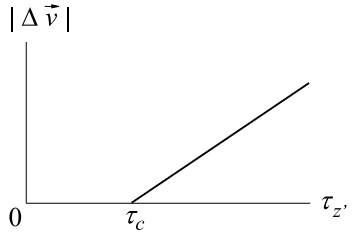

Fig. 2. The relative speed $|\Delta\vec{v}|$ of two adjacent grains is proportional to the shear stress $\tau_{z'}$ resolved in the plane of the grain boundary shared by the two grains, when greater than the critical stress τ_c. Otherwise the relative speed vanishes.

As $\Delta\vec{v}$ is parallel to the shear force in the plane of the interface, its components are given by $\Delta v_{i'} = Q(\tau_{z'} - \tau_c)(\sigma_{i'z'}/\tau_{z'})$, $i' = x', y'$, for $\tau_{z'} \geq \tau_c$. This expression for $\Delta\vec{v}$ has proven to hold with great accuracy for several aluminium, titanium and magnesium alloys [4,5,3]. Hence the force law at the grain scale takes the general form

$$\Delta v_{i'} = \begin{cases} Q\left(1 - \dfrac{\tau_c}{\tau_{z'}}\right)\sigma_{i'z'}, & i' = x', y', \text{ if } \tau_{z'} > \tau_c \\ 0, & \text{otherwise,} \end{cases} \qquad (1)$$

$$\Delta v_{z'} \equiv 0.$$

The coefficient $Q = Q(p, T)$ does not depend on the shear stresses and neither on the orientation of the grain boundary, therefore its dependence on the normal stresses is only via the hydrostatic pressure invariant $p = -(\sigma_{x'x'} + \sigma_{y'y'} + \sigma_{z'z'})/3$. Here T denotes the absolute temperature.

The next two steps are, on the one hand, to express the grain scale force law (1) in the frame of reference (xyz), common to all the grain surfaces, instead of the local ones $(x'y'z')$. Given the rotation matrix $R(\theta, \phi) = (R_{ij}(\theta, \phi))$ connecting the two frames of reference one can put the local stress tensor

$$(\sigma_{i'j'}) = R(\theta, \phi)(\sigma_{ij})R^T(\theta, \phi) \qquad (2)$$

in terms of the stress tensor (σ_{ij}) of the externally applied forces and the Euler angles (θ, ϕ) of the grain boundary plane. The macroscopic equations of motion are obtained from replacing the result in Eq. (1) and then averaging over the Euler angles. The second step in reformulating Eq. (1) is to put it in terms of the strain tensor and its time derivative instead of the relative velocity between adjacent grains.

3. The equations of motion in the plastic flow

3.1. Stress and the relative velocity between adjacent grains

A detailed account of the procedure outlined above can be found in the literature on superplasticity [2,4,5,3,38]. Specifically, section 2 of Ref. [3] gives a complete account of the program outlined in the last paragraph of the preceding section. However, the analysis of the general equations and discussions given there focuses on just the superplastic solutions [4,5]. We recall here the results already given in the just cited literature to make apparent that superplastic and normal ductile behaviour are two regimes which are inferred from the same mathematical scheme. Some derivations taken from already published papers will be reviewed next in the interest of completeness.

Assuming the important special case of an externally applied unidirectional normal stress σ along the $z-$axis on a polycrystalline solid, isotropic in the scale much larger than the mean grain size d, the stress tensor reads

$$(\sigma_{ij}) = \begin{pmatrix} \sigma_\perp & 0 & 0 \\ 0 & \sigma_\perp & 0 \\ 0 & 0 & \sigma \end{pmatrix}. \qquad (3)$$

A non–vanishing transversal stress $\sigma_\perp$ is assumed because it will be demonstrated that plastic strain always induces such kind of stress. Settling the transversal stress to zero may be acceptable as a circumstance occurring at a given time, but may yield gross errors if taken as a permanent condition when the mechanical analysis incorporates de possibility of plastic flow. Writing $\sigma_\perp$ in terms of the hydrostatic pressure p it reads

$$\sigma_\perp = -\frac{1}{2}(\sigma + 3p). \qquad (4)$$

The local $(x'y'z')$ frame must be chosen so that the unit vector $\hat{k}'$ along the $z'-$axis be normal to the plane of the shared grain surface. The other two axes can be taken in the most convenient way and hence the $x'-$axis will be selected as the intersection of the $x'y'$ and xy planes. Calling ϕ the Euler angle between the x and x' axes, and θ the Euler angle going from the z to the z' axis, the rotation matrix takes the general form

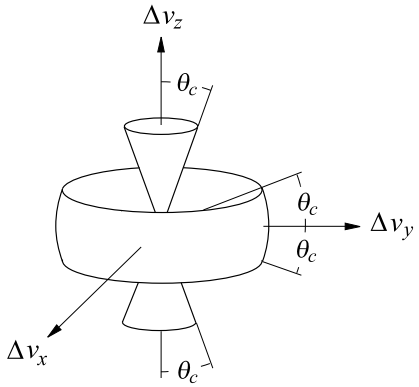

Fig. 3. The critical angle θ_c for a solid undergoing plastic strain in the direction of the z–axis. Adjacent grains whose common boundary has the normal inside the solid angles around the z–axis and the xy–plane are impeded to slide by the condition (8). The axes are in the principal directions of the stress tensor and θ_c is defined by Eq. (9).

$$R(\theta,\phi)=\begin{pmatrix}\cos\phi & \sin\phi & 0\\ -\sin\phi\cos\theta & \cos\phi\cos\theta & \sin\theta\\ \sin\phi\sin\theta & -\cos\phi\sin\theta & \cos\theta\end{pmatrix}. \tag{5}$$

Replacing (σ_{ij}) and $R(\theta,\phi)$, as given by Eqs. (3) and (5), into Eq. (2) one obtains the rotated stress tensor

$$(\sigma_{i'j'})=\begin{pmatrix}\sigma_\perp & 0 & 0\\ 0 & \sigma\sin^2\theta+\sigma_\perp\cos^2\theta & (\sigma-\sigma_\perp)\sin\theta\cos\theta\\ 0 & (\sigma-\sigma_\perp)\sin\theta\cos\theta & \sigma\cos^2\theta+\sigma_\perp\sin^2\theta\end{pmatrix}.$$

Thus, recalling Eq. (4), one can write the components of the shear stress on the intergrain surface as

$$\sigma_{x'z'}=0,\quad \sigma_{y'z'}=\frac{3}{2}(\sigma+p)\sin\theta\cos\theta.$$

With these results Eqs. (1) can be put in explicit form in the main frame of reference (xyz). The relative velocity $\Delta\vec{v}$ between two adjacent grains turns out to be

$$\Delta\vec{v}=\frac{3}{2}\mathcal{Q}(\sigma+p)\sin\theta\cos\theta\left(1-\frac{2\tau_c}{3|(\sigma+p)\sin\theta\cos\theta|}\right)\hat{v}, \tag{6}$$

where the unit vector $\hat{v}$ is the vector $\hat{j}'$ along the y'–axis. To express it in the main frame of reference we have to solve

$$\hat{v}=\hat{j}'=R^T(\theta,\phi)\begin{pmatrix}0\\1\\0\end{pmatrix}$$

which, with help of Eq. (5), yields

$$\hat{v}=(-\sin\phi\cos\theta,\cos\phi\cos\theta,\sin\theta). \tag{7}$$

Eq. (6) holds whenever

$$\left|\frac{3}{2}(\sigma+p)\sin\theta\cos\theta\right|>\tau_c, \tag{8}$$

otherwise $\Delta\vec{v}=0$. By the choice of the x' axis in the xy plane any direction in the xy plane is a principal direction and then $\sigma_{x'z'}=0$ for any θ and ϕ.

Condition (8) is fulfilled whenever $\theta\le\theta_c$, where θ_c is a critical angle given by

$$\sin(2\theta_c)=\frac{4\tau_c}{3|\sigma+p|}. \tag{9}$$

Eq. (8) has a major effect in the plastic regime of deformation, which is quite easy to understand from just phenomenological arguments. No matter how strong the applied external forces may be, the shear stress vanishes in planes normal to the principal directions of the stress tensor. Hence, a grain boundary whose normal is close enough to a principal direction is impeded to slide because, by continuity, the magnitude of the shear stress in it is smaller than τ_c. Fig. 3 shows how this effect takes place in an axially symmetric medium. This effect shows that a continuous medium constituted by random polyhedra, leaving no voids between them, cannot be taken as an homogeneous and isotropic medium, irrespectively of how small and randomly oriented the polyhedra may be.

3.2. Velocity field, strain rate and stress tensors

The proper configuration variables in the macroscopic scale are the components ε_{ij} $(i,j=x,y,z)$ of the strain tensor, which, together with their time derivatives $\dot{\varepsilon}_{ij}$ give a complete description of the dynamical state of the system. Alternatively, when dealing with the material medium as a flowing continuum the proper variable to characterize the dynamical state is the velocity field $\vec{v}(\vec{r},t)$. The two pictures are related by

$$\dot{\epsilon}_{ij}=\frac{1}{2}\left(\frac{\partial v_i}{\partial x_j}+\frac{\partial v_j}{\partial x_i}\right),\quad i,j=x,y,z \text{ or } x_j=x,y,z\,. \tag{10}$$

The first step to put the force law (1) between the elementary constituents in terms of the macroscopic variables at any point of the material medium is to find out the connection between the relative velocities $\Delta\vec{v}$ of adjacent grains and the velocity field $\vec{v}$ they give rise. To this aim consider first two points at (x,y,z) and $(x+\delta x,y,z)$ inside a polycrystalline material, where the coordinates are referred to the main frame of reference (xyz), common to all grains. Though small, the segment δx intersects a large number n of grain boundaries, and hence $\delta x=nd$, where d is the averaged grain size. The relative velocity between the two extreme points of the segment δx is the sum of all the n relative velocities between the consecutive grains. Therefore,

$$\frac{\vec{v}(x+\delta x,y,z)-\vec{v}(x,y,z)}{\delta x}=\frac{1}{nd}\sum_{k=1}^{n}\Delta\vec{v}(k), \tag{11}$$

where k numbers the succession of intersected grain boundaries. But for the factor d in the denominator, the right hand side of this equation defines the mean value of the grain relative velocities along the x–axis

$$\frac{1}{nd}\sum_{k=1}^{n}\Delta\vec{v}(k)=\frac{1}{d}\langle\Delta\vec{v}\rangle_x. \tag{12}$$

Thus, in the proper limit,

$$\frac{\partial v_i}{\partial x_j}=\frac{1}{d}\langle\Delta v_i\rangle_j,\quad i,j=x,y,z \text{ or } x_j=x,y,z\,, \tag{13}$$

where symbol $\langle\dots\rangle_j$ means the average over all boundary orientations along the x_j axis in the positive sense. The dependence on j in the right hand side of Eq. (13) denotes the direction along which the relative velocities are sampled, which in Eqs. (11) and (12) is simply the x direction.

A complete set of equations for the velocity field $\vec{v}(x,y,z)$ of the material medium can be derived from solving the mean values appearing in the right hand side of Eq. (13), which assumes that the mean grain size d is conserved. The so obtained equations, relating $\partial v_i/\partial x_j$ with the stresses, can be combined to form rotation invariants like $\nabla\cdot\vec{v}$ and $\nabla\times\vec{v}$, or the components of the strain rate tensor by means of Eq. (10).

The normals to the boundaries shared by adjacent grains along a given coordinate axis x_j are oriented at random. Hence the summation along a number of successive inter–grain surfaces can be carried out by averaging over all the permissible orientations, disregarding the spatial shift between the grain boundaries. Then the mean value appearing in Eq. (13) can be written as

$$\langle\Delta\vec{v}\rangle_j=\frac{1}{2\pi}\int_{D_j}d\phi\,d\theta\,\sin\theta\Delta\vec{v}(\theta,\phi), \tag{14}$$

where the integration domains D_j are determined by the condition $|\sin\theta|>\sin\theta_c$ and z' in the semi-space $x_j\geq 0$. (The average considers only a semi–space because the strain components have implicit the two sides of the volume element.) Explicitly, the integration domains are

$$\begin{aligned}
&D_x:\ \theta\in[\theta_c,\pi/2-\theta_c]\cup[\pi/2+\theta_c,\pi-\theta_c],\\
&\qquad\phi\in[0,\pi],\\
&D_y:\ \theta\in[\theta_c,\pi/2-\theta_c]\cup[\pi/2+\theta_c,\pi-\theta_c],\\
&\qquad\phi\in[\pi/2,3\pi/2],\\
&D_z:\ \theta\in[\theta_c,\pi/2-\theta_c],\\
&\qquad\phi\in[0,2\pi].
\end{aligned} \tag{15}$$

The integrals (14) can be solved exactly. Combining Eqs. (6) and (7)

$$\Delta v_x=-\frac{3}{2}\mathcal{Q}(\sigma+p)\left[\sin\theta\cos^2\theta\sin\phi-\frac{2\tau_c}{3|\sigma+p)|}\cos\theta\sin\phi\right],$$

$$\Delta v_y=\frac{3}{2}\mathcal{Q}(\sigma+p)\left[\sin\theta\cos^2\theta\cos\phi-\frac{2\tau_c}{3|\sigma+p|}\cos\theta\cos\phi\right],$$

$$\Delta v_z = \frac{3}{2}Q(\sigma+p)\left[\sin^2\theta\cos\theta - \frac{2\tau_c}{3|\sigma+p|}\sin\theta\right],$$

replacing this into Eq. (14), integrating over the domains (15) and recalling Eqs. (10) and (13), it is obtained that

$$\dot{\epsilon}_{xx} = \dot{\epsilon}_{yy} = -\frac{3}{16d}Q(\sigma+p)\left[1 - \frac{4\theta_c}{\pi} + \frac{\sin(4\theta_c)}{\pi}\right] + s\frac{Q\tau_c}{d}\frac{\cos(2\theta_c)}{\pi}, \tag{16}$$

$$\dot{\epsilon}_{zz} = \frac{3}{8d}Q(\sigma+p)\cos(2\theta_c) - s\frac{Q\tau_c}{d}\left(\frac{\pi}{4} - \theta_c\right), \tag{17}$$

where s is the sign $s = (\sigma+p)/|\sigma+p|$.

3.3. Hooke's law and the plastic regime of deformation

Of special importance for the derivations what follows is a modality of Hooke's law valid when a solid material is being plastically deformed. We spend some space next to explain a conception which, though not complex, may sound rather odd when mentioned in this context. Hooke's law is often invoked when studying the elastic deformation of solids, but rarely when dealing with their plastic flow. However, elastic deformations at each of the many elements of matter constituting a body are still present when flowing plastically.

Take for instance a rectangular hexahedron of volume $\Delta V = \Delta x\Delta y\Delta z$, being Δx, Δy, Δz the edges. After a deformation $\Delta x \to \Delta x + \delta\Delta x$, $\Delta y \to \Delta y + \delta\Delta y$, $\Delta z \to \Delta z + \delta\Delta z$, up to the first order in the edge variations the volume change per unit volume is

$$\frac{\delta\Delta V}{\Delta V} = \frac{\delta\Delta x}{\Delta x} + \frac{\delta\Delta y}{\Delta y} + \frac{\delta\Delta z}{\Delta z}. \tag{18}$$

In a time dependent scheme the relative velocity between two opposite faces of the hexahedron, interpreted now as an elementary piece of matter of a deforming solid, is $(\partial v_i/\partial x_i)\Delta x_i$. Hence, in a time interval δt their distance increases in

$$\delta\Delta x_i = \frac{\partial v_i}{\partial x_i}\Delta x_i\,\delta t, \quad x_i = x,\, y,\, z.$$

Recalling Eq. (18) and combining this simple geometric observation with Eq. (10) one can deduce that the local time rate of volume variation per unit volume of the deforming material is

$$\frac{\dot{V}}{V} = \nabla\cdot\vec{v} = \dot{\epsilon}_{xx} + \dot{\epsilon}_{yy} + \dot{\epsilon}_{zz}.$$

Hooke's law $B(\Delta V/V) = p$, where B is the bulk modulus, relates the hydrostatic pressure p with the volume variation $\Delta V/V$ per unit volume, no matter the mechanical process the material may be going through. In our case Hooke's law takes the form $\dot{p} = B(\dot{V}/V)$ where, as usual, the dots indicate time derivatives. Combining this with Eqs. (16) and (17) we have that

$$\dot{p} = sB\frac{\tau_c Q}{2d}\left[\frac{1-\cos(2\theta_c)}{\sin(2\theta_c)} - 2\theta_c\left(1 + \frac{2}{\pi\sin(2\theta_c)}\right) - \frac{2}{\pi}\cos(2\theta_c) + \frac{\pi}{2}\right], \tag{19}$$

which, together with the equation

$$\dot{\epsilon} = s\,\frac{\tau_c Q}{2d}\left[\cot(2\theta_c) + 2\theta_c - \frac{\pi}{2}\right] \tag{20}$$

for the axial strain $\epsilon \equiv \epsilon_{zz}$, constitute the force laws in the macroscopic scale. Eqs. (19) and (20) were written in terms of θ_c just for brevity. Recalling its definition (9) the state variables turn out to be the axial stress σ, the axial strain ϵ, and the hydrostatic pressure p.

The relevant role of p in the plastic deformation of polycrystalline solids may seem quite amazing, however it explains a number of properties specific to this kind of physical processes. Bauschinger effect is one of them: the time dependent plastic flow is determined by the initial value of p, which is difficult to measure and is in most cases disregarded, attributing its effect to a dependence on history of the structure of the material.

3.4. The coefficient Q

The properties of the specific material enter the theoretical formulation through the coefficient $Q(p,T)$, where T is the temperature, governing grain boundary sliding. It has been studied in detail for fine grained polycrystalline solids and has been shown to be of the general form [3,38,36,41,40]

$$\frac{Q}{4d} = C_0\frac{\Omega^*}{k_B T}\exp\left(-\frac{\epsilon_0 + \Omega^* p}{k_B T}\right), \tag{21}$$

where k_B is the Boltzmann constant, the coefficient C_0 depends only on the grain size d, the constant ϵ_0 is the energy necessary for evaporating a crystal vacancy from the grain boundary, and Ω^* is the excitation volume for the same process. The major role played

in grain sliding by the exchange of crystal vacancies between the grains and their boundaries has been evidenced both theoretical [38,40] and experimentally [41].

Eqs. (19), (20) and (9) show that plastic flow is essentially a time dependent problem. They govern the coupled time evolution of the three variables, σ, ε and p, relevant for the cylindrically symmetric deformation of a polycrystalline continuous medium. The actual behaviour of these variables in specific circumstances depends also on the initial conditions and deformation path (either $\sigma =$ constant, $\dot{\varepsilon} =$ constant, or any other imposed condition between the variables and their time derivatives). The initial conditions should include the usually ignored variable p [39]. One can set the transversal stress $\sigma_\perp = -(\sigma + 3p)/2 = 0$ as a natural initial condition if the material has been previously annealed, but $\sigma_\perp$ is expected to take finite values in the subsequent deformation, evolving in time as dictated by the equations of motion. The plastic stretching in one direction is always accompanied by a finite compression $\sigma_\perp$ in the plane normal to the deformation axis, which increases monotonically with strain. This explains why necking always precedes ductile fracture [39].

4. Plastic deformation at constant strain rate $\dot{\varepsilon}$

At constant temperature T the coefficient Q depends only on the hydrostatic pressure p. Reordering Eq. (20) in order to isolate Q in the left hand side of the equation, and then derivating with respect to p, with $\dot{\varepsilon}$ constant, one readily shows that

$$-\frac{\dot{\varepsilon} d}{\tau_c}\frac{1}{Q^2}\frac{dQ}{dp} = \left[-\frac{1}{\sin^2(2\theta_c)} + 1\right]\frac{d\theta_c}{dp}.$$

Replacing next in this result Q, as given by Eq. (21), it follows that

$$\frac{dp}{Q} = -s\frac{\tau_c k_B T}{\Omega^* \dot{\varepsilon} d}\cot^2(2\theta_c)\, d\theta_c. \tag{22}$$

Dividing Eq. (20) by Eq. (19), inserting the result in the identity $d\varepsilon = (\dot{\varepsilon}/\dot{p})\, dp$, using Eq. (22) to substitute the differential dp by $d\theta_c$, and then integrating, it is obtained that

$$\varepsilon = -\frac{2k_B T}{\Omega^* B}\int_{\theta_0}^{\theta_c} d\theta\, \cot^2(2\theta)\left[\frac{1-\cos(2\theta)}{\sin(2\theta)} - 2\theta\left(1 + \frac{2}{\pi\sin(2\theta)}\right) - \frac{2}{\pi}\cos(2\theta) + \frac{\pi}{2}\right]^{-1}.$$

The lower integration limit θ_0 incorporates the initial conditions. When the material has been previously submitted to a stress relieving heat treatment, the initial conditions are $\sigma_\perp = 0$ and $\sigma = \sigma_0$, being σ_0 the initially applied axial stress. The initial pressure is then $p_0 = -\sigma_0/3$. In such situation

$$\theta_0 = \frac{1}{2}\arcsin\frac{2\tau_c}{|\sigma_0|}.$$

The upper limit is given by the final stress σ and hydrostatic pressure p

$$\theta_c = \frac{1}{2}\arcsin\frac{2\tau_c}{|\sigma + p|}.$$

Defining the universal function $F(\theta)$ as the indefinite integral

$$F(\theta) = -2\int d\theta\, \cot^2(2\theta)\left[\frac{1-\cos(2\theta)}{\sin(2\theta)} - 2\theta\left(1 + \frac{2}{\pi\sin(2\theta)}\right) - \frac{2}{\pi}\cos(2\theta) + \frac{\pi}{2}\right]^{-1},$$

the expression for the strain reads

$$\varepsilon = \frac{k_B T}{B\Omega^*}[F(\theta_c) - F(\theta_0)], \quad (\dot{\varepsilon} = \text{ constant}). \tag{23}$$

Fig. 4 shows the function $F(\theta)$ with the arbitrary constant chosen so that $F(0.8) = 0$.

5. Plastic and superplastic solutions

As shown in Fig. 2, $F(\theta)$ is monotonically decreasing in its whole range $(0, \pi/4)$ and has two singularities, at $\theta = 0$ and $\theta = \pi/4$. If the material has been thoroughly annealed for removing any residual internal stress prior to the plastic deformation, it holds the initial condition $p = -\sigma_0/3$ at $\varepsilon = 0$, where σ_0 is the stress at the beginning of the plastic deformation.

The magnitude of ε is controlled by the adimensional coefficient appearing in Eq. (23), which is a very small quantity. The bulk modulus B for metals is of the order of 10^{11} Pa. Previous literature on aluminium and titanium alloys shows that Ω^* is $2.6\times10^{-27}\,\mathrm{m}^3$ for Al–8090 and $5.9\times10^{-28}\,\mathrm{m}^3$ for titanium Ti–6Al–4V at rather high temperatures [3]. Assuming Ω^* does not vary too much with T one can take these figures to estimate that, at $T = 300\,\mathrm{K}$,

$$\frac{k_B T}{B\Omega^*} \sim 2.3 - 7.0\times10^{-5}. \tag{24}$$

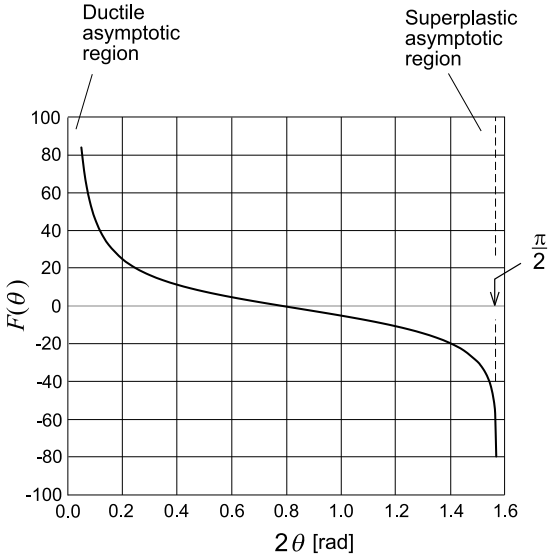

Fig. 4. The universal function $F(\theta)$ showing the two singularities, corresponding to superplastic and normal ductility regimes.

Because of the small value of the coefficient (24), any significant strain ε demands that the function $F(\theta)$ be large, of the order of 10^3, to have a strain of a few percents. Hence θ_0, or θ_c, or both, must be in one of the two asymptotic regions $\theta \gtrsim 0$ or $\theta \lesssim \pi/4$. The threshold stress τ_c for grain sliding of superplastic materials at high temperatures is generally in the range $0.5 - 5\,\mathrm{MPa}$ For ductile materials the figures are somewhat higher, of the order of twice the CRSS, which may be of the order of 20–25 MPa, as is the case of iron at normal temperature. Anyway we can consider τ_c as much smaller than the applied stresses σ that are customary in mechanical tests. Hence the divergence at $\theta = 0$ should be the right one for ductile plastic distortion, and appreciable strains occur for

$$\theta_c(\varepsilon, \dot{\varepsilon}, T) \approx 0. \tag{25}$$

The other pole of function $F(\theta)$ corresponds to very slow flux, as occurring in superplastic deformation, and has been extensively studied in the literature.

6. Ductile deformation, necking and strain to fracture

Making the quotient between Eqs. (19) and (20) one has that

$$\frac{dp}{d\varepsilon} = sB\frac{\tau_c Q}{2\dot{\varepsilon}d}\left[\frac{1-\cos(2\theta_c)}{\sin(2\theta_c)} - 2\theta_c\left(1+\frac{2}{\pi\sin(2\theta_c)}\right) - \frac{2}{\pi}\cos(2\theta_c) + \frac{\pi}{2}\right]. \tag{26}$$

To materialize the asymptotic limit (25), just terms up to the first order in θ are retained in this equation. The expression in between the square brackets in Eq. (26) reduces to $\pi/2 - 4/\pi - \theta$. The constant $\pi/2 - 4/\pi = 0.29756$ is not small enough and we can neglect θ when compared with it. Thus, with no significant loss of precision the exact equation can be reduced to the much simpler first order differential equation

$$\frac{dp}{d\varepsilon} = s\left(\pi - \frac{8}{\pi}\right)\frac{C_0 B\tau_c\Omega^*}{k_B T\dot{\varepsilon}}\exp\left(-\frac{\epsilon_0 + \Omega^* p}{k_B T}\right),$$

whose solution can be written as

$$p - p_0 = \frac{k_B T}{\Omega^*}\ln\left[1 - C_0\frac{\pi^2-8}{\pi}\frac{\tau_c B}{\dot{\varepsilon}}\left(\frac{\Omega^*}{k_B T}\right)^2\exp\left(-\frac{\epsilon_0 + \Omega^* p_0}{k_B T}\right)|\varepsilon|\right], \tag{27}$$

where it was substituted $s\varepsilon = |\varepsilon|$.

Eq. (27) expresses a main finding of this work: when the modulus $|\varepsilon|$ of the strain approaches from below the value

$$\varepsilon_{\mathrm{frac}} = \frac{\pi\dot{\varepsilon}}{(\pi^2-8)C_0\tau_c B}\left(\frac{k_B T}{\Omega^*}\right)^2\exp\left(\frac{\epsilon_0 + \Omega^* p_0}{k_B T}\right) \tag{28}$$

the hydrostatic pressure p diverges logarithmically. According to the definition of p, positive stresses (tension) contribute negatively to the hydrostatic pressure p. If the sample is conveniently annealed prior to the tensile test then $p_0 = -\sigma_0/3$, where σ_0 is the applied initial tensile stress. As the test proceeds, $p = -(\sigma + 2\sigma_\perp)/3$ increases monotonically with ε, and the transversal stress $\sigma_\perp$ increases

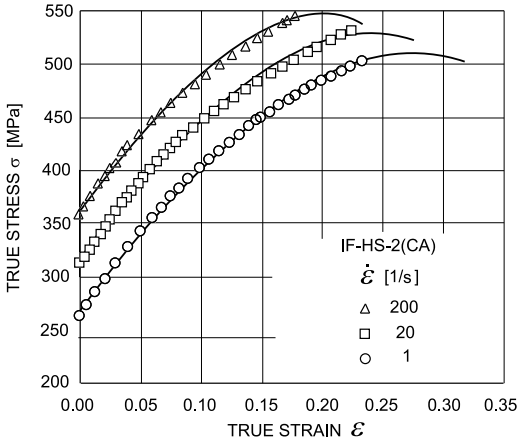

Fig. 5. Circles represent the stress–strain experimental data for a copper–alloyed high–strength interstitial free steel at the three strain rates shown in the inset [42]. The continuous lines represent the predictions of Eq. (23) with the parameters optimizing the fit to the experimental points, shown in Table 1.

Table 1
Values for the parameters giving the fits of Fig. 5.

$\dot{\epsilon}$ [s^{-1}]	σ_0 [MPa]	$\frac{B\Omega^*}{k_BT}\tau_c$ [MPa]	$\frac{k_BT}{\Omega^*}$ [MPa]	$\varepsilon_{\text{frac}}$
200	362	6805	457	0.370
20	318	9704	1440	0.615
1	268	10511	1980	0.750

from zero to negative (compressive) values. When ε approaches the critical value $\varepsilon_{\text{frac}}$ the transversal stress $\sigma_\perp$ increases very rapidly, producing the characteristic neck and fracture. Therefore, Eq. (28) for $\varepsilon_{\text{frac}}$ expresses the strain to fracture of the material.

Eq. (28) gives the strain to fracture in terms of the constants of the theory. However one can express it in terms of more standard coefficients and easily measurable quantities. Combining Eqs. (20) and (21), and taking into account the asymptotic approximation (25) to write

$$\cot(2\theta_0) + 2\theta_0 - \frac{\pi}{2} \approx \frac{1}{2\theta_0} \approx \frac{\sigma_0}{2\tau_c},$$

Eq. (28) can be written as

$$\varepsilon_{\text{frac}} = \frac{\pi}{(\pi^2 - 8)} \frac{k_BT}{B\Omega^*} \frac{\sigma_0}{\tau_c} \tag{29}$$

and the strain becomes given by Eq. (30) below

$$\sigma = \sigma_0 + \frac{2}{3}\left(\pi - \frac{8}{\pi}\right)\frac{B\Omega^*\tau_c}{k_BT}\varepsilon + \frac{k_BT}{\Omega^*}\ln\left(1 - \frac{\varepsilon}{\varepsilon_{\text{frac}}}\right). \tag{30}$$

We recall that σ_0 is the stress registered when the plastic deformation at the chosen constant strain rate $\dot{\epsilon}$ begins. The bulk modulus B is in tables and the only undetermined parameter is the product $\Omega^*\tau_c$. However, $\Omega^*\tau_c$ can be determined independently from other features of the plastic deformation of the sample in order to have a parameter free test of Eq. (28). To show how well this expression compares with experiment, we include next a study of a representative commercial steel.

As a representative example, Fig. 5 shows the results of a mechanical test of a copper–alloyed high–strength interstitial free steel at strain rates 1, 20 and 200 s^{-1} [42], together with the fits of Eq. (23) with the asymptotic approximation (25). The high quality of the agreement between theory and experiment is apparent in the figure, and the very little dispersion of the fitting parameters $\Omega^* B$ and τ_c shown in Table 1 reinforces this perception. The last column of Table 1 displays the strain to failure $\varepsilon_{\text{frac}}$ for the three strain rates, as given by Eq. (29) where the parameters appearing in the left side of Table 1 were substituted. The values are very close to those measured in the mechanical testings. Comparisons between predicted strains to fracture with published results of experimental tests for many other commercial alloys exhibit same agreement as the one shown in Fig. 5 and Table 1.

Although the existence of cracks and imperfections inside a stressed solid may contribute to accelerate fracture, the general cause of ductile fracture is not in them. An ideal fine–grained polycrystalline material, free of voids and cracks, whose grains are prone to slide, readily accommodating each other's shapes, inevitably should fail after a finite plastic strain.

7. Final remarks

The preceding sections show that plastic flow governed by the ductile pole of the universal function $F(\theta)$ should end in fracture, without the intervention of voids and cracks. Fracture occurs at a precise strain, for which the hydrostatic pressure diverges when the solid is in the plastic regime associated to the pole at $\theta = 0$ of the universal function $F(\theta)$. The effect is essentially dynamic and caused by the faceted geometry of the grains. When dealing with the static properties in a scale much larger than the grain sizes, the polycrystal can be taken in the average as an isotropic homogeneous medium. However, this picture ceases to be valid when the material flows. The faceted nature of the elementary constituents has a macroscopic effect no matter how small the grains may be.

The hypotheses employed here are not contradictory with previous studies attributing fracture to the nucleation, growing and coalescence of voids, because predict simply an alternate self–consistent mechanism. The model is consistent also with the standard theory of plasticity [21]. In effect, notice that Eqs. (4) of Ref. [39] reduce to

$$\frac{\dot{\epsilon}_{xx}}{\sigma_{xx}+p} = \frac{\dot{\epsilon}_{yy}}{\sigma_{yy}+p} = \frac{\dot{\epsilon}_{zz}}{\sigma_{zz}+p} \tag{31}$$

because in the asymptotic approximation $\theta_c \approx 0$ used here one has that $f_s(2\theta_c) = g_s(2\theta_c)$. Eqs. (30) are the well–known Lévy–Mises equations. Also Eq. (5) of Ref. [39] is the von Mises yield criterion with von Mises yield stress

$$\sigma_Y = 2\tau_c.$$

Hence the Lévy–Mises equations and von Mises yield criterion are rigorously demonstrated in the theoretical scheme used here.

Funding statement

This research did not receive any specific grant from funding agencies in the public, commercial, or non-profit sectors.

CRediT authorship contribution statement

Miguel Lagos: Writing – review & editing, Supervision, Methodology, Investigation. **César Retamal:** Writing – original draft, Supervision, Methodology, Investigation. **Rodrigo Valle:** Writing – original draft, Methodology, Investigation, Formal analysis. **Rodrigo Paredes:** Writing – original draft, Software, Investigation, Data curation, Conceptualization.

Declaration of competing interest

The authors declare that they have no known competing financial interests or personal relationships that could have appeared to influence the work reported in this paper.

References

[1] E. Orowan, Fracture and strength of solids, Rep. Prog. Phys. 12 (1949) 185.
[2] M. Lagos, Theory of superplasticity in polycrystalline materials: stress-induced structural instabilities of grain boundaries, Phys. Rev. B 71 (2005) 224117.
[3] M. Lagos, Theory of ductility: from brittle to superplastic behavior of polycrystals, Phys. Rev. B 73 (2006) 224107.
[4] M. Lagos, C. Retamal, Grain dynamics and plastic properties of highly refined materials, Phys. Scr. 82 (2010) 065603.
[5] M. Lagos, C. Retamal, A theoretical approach to finite strain superplasticity and some of its applications, Phys. Scr. 81 (2010) 055601.
[6] E. Maire, O. Bouaziz, M. Di Michiel, C. Verdu, Initiation and growth of damage in a dual-phase steel observed by X-ray microtomography, Acta Mater. 56 (2008) 4954.
[7] L. Lecarme, C. Tekoğlu, T. Pardoen, Void growth and coalescence in ductile solids with stage III and stage IV strain hardening, Int. J. Plast. 27 (2011) 1203.
[8] L. Lecarme, E. Maire, A. Kumar K.C., C. De Vleeschouwer, L. Jacques, A. Simar, T. Pardoen, Heterogenous void growth revealed by in situ 3-D X-ray microtomography using automatic cavity tracking, Acta Mater. 63 (2014) 130.
[9] C.C. Roth, T.F. Morgeneyer, Y. Cheng, L. Helfen, D. Mohr, Ductile damage mechanism under shear-dominated loading: in–situ tomography experiments on dual phase steel and localization analysis, Int. J. Plast. 109 (2018) 169.
[10] A. Weck, D.S. Wilkinson, Experimental investigation of void coalescence in metallic sheets containing laser drilled holes, Acta Mater. 56 (2008) 1774.
[11] A.A. Griffith, The phenomenon of rupture and flow in solids, Philos. Trans. R. Soc. Lond. A 221 (1921) 163.
[12] G.R. Irwin, in: Fracturing of Metals, American Society of Metals, Cleveland, OH, 1948, p. 147.
[13] I. Kolvin, J. Fineberg, M. Adda-Bedia, Nonlinear focusing in dynamic crack fronts and the microbranching transition, Phys. Rev. Lett. 119 (2017) 215505.
[14] I. Svetlizky, E. Bayart, G. Cohen, J. Fineberg, Frictional resistance within the wake of frictional rupture fronts, Phys. Rev. Lett. 118 (2017) 234301.
[15] S.I. Heizler, D.A. Kessler, Three-dimensional to two–dimensional transition in mode-I fracture microbranching in a perturbed hexagonal close-packed lattice, Phys. Rev. E 95 (2017) 063004.
[16] J. Fineberg, E. Bouchbinder, Recent developments in dynamic fracture: some perspectives, Int. J. Fract. 196 (33) (2015).
[17] A.L. Gurson, Continuum theory of ductile rupture by void nucleation and growth part I–yield criteria and flow rules for porous ductile media, J. Eng. Mater. Technol. Trans. ASME 99 (2) (1977).
[18] V. Tvergaard, On localization in ductile materials containing spherical voids, Int. J. Fract. 18 (1982) 237.
[19] V. Tvergaard, A. Needleman, Analysis of the cup–cone fracture in a round tensile bar, Acta Metall. 32 (1984) 157.
[20] V. Tvergaard, Material failure by void growth to coalescence, Adv. Appl. Mech. 27 (1989) 83–151.
[21] A.S. Khan, S. Huang, Continuum Theory of Plasticity, John Wiley & Sons. INC., New York, 1995.
[22] J. Lemaitre, A continuous damage mechanics model for ductile fracture, J. Eng. Mater. Technol. Trans. ASME 107 (83) (1985).
[23] Z.L. Zhang, C. Thaulow, J. Odegard, A complete Gurson model approach for ductile fracture, Eng. Fract. Mech. 67 (2000) 155.
[24] K. Nahshon, J.W. Hutchinson, Modification of the Gurson model for shear failure, Eur. J. Mech. A, Solids 27 (1) (2008).

[25] L. Xue, Constitutive modeling of void shearing effect in ductile fracture of porous materials, Eng. Fract. Mech. 75 (2008) 3343.
[26] A.V. Shutov, C.B. Silbermann, J. Ihlemann, Ductile damage model for metal forming simulations including refined description of void nucleation, Int. J. Plast. 71 (2015) 195.
[27] H. Li, M.W. Fu, J. Lu, H. Yang, Ductile fracture: experiments and computations, Int. J. Plast. 27 (2011) 147.
[28] P.J. Noell, J.D. Carroll, B.L. Boyce, The mechanisms of ductile rupture, Acta Mater. 161 (83) (2018).
[29] G. Rousselier, Ductile fracture models and their potential in local approach of fracture, Nucl. Eng. Des. 105 (97) (1987).
[30] G. Rousselier, Dissipation in porous metal plasticity and ductile fracture, J. Mech. Phys. Solids 49 (2001) 1727.
[31] G. Rousselier, S. Leclercq, A simplified “polycrystalline” model for viscoplastic and damage finite element analyses, Int. J. Plast. 22 (2006) 685.
[32] G. Rousselier, M. Luo, A fully coupled void damage and Mohr–Coulomb based ductile fracture model in the framework of a reduced texture methodology, Int. J. Plast. 55 (1) (2014).
[33] A.S. Khan, S. Yu, Deformation induced anisotropic responses of Ti–6Al–4V alloy. Part I: experiments, Int. J. Plast. 38 (1) (2012).
[34] A.S. Khan, S. Yu, H. Liu, Deformation induced anisotropic responses of Ti–6Al–4V alloy. Part II: a strain rate and temperature dependent anisotropic yield criterion, Int. J. Plast. 38 (14) (2012).
[35] A.S. Khan, H. Liu, A new approach for ductile fracture prediction on Al 2024-T351 alloy, Int. J. Plast. 35 (1) (2012).
[36] Y. Qi, P.E. Krajewski, Molecular dynamics simulations of grain boundary sliding: the effect of stress and boundary misorientation, Acta Mater. 55 (2007) 1555.
[37] P. Bellon, R.S. Averback, Nonequilibrium roughening of interfaces in crystals under shear: application to ball milling, Phys. Rev. Lett. 74 (1995) 1819.
[38] M. Lagos, Elastic instability of grain boundaries and the physical origin of superplasticity, Phys. Rev. Lett. 85 (2000) 2332.
[39] M. Lagos, V. Conte, Mathematical model for the plastic flow of a polycrystalline material medium, Scr. Mater. 65 (2011) 1053.
[40] M. Lagos, H. Duque, Two–phase theory for the superplastic flow, Int. J. Plast. 17 (2001) 369.
[41] J.S. Vetrano, E.P. Simonen, S.M. Bruemmer, Acta Mater. 47 (1999) 4125.
[42] R. Rana, S. Singh, W. Bleck, O. Mohanty, Effect of Temperature and Dynamic Loading on the Mechanical Properties of Copper-Alloyed High–Strength Interstitial–Free Steel, The Minerals, Metals & Materials Society and ASM International, 2009.